Korean J. Chem. Eng., **28**(11), 2178-2183 (2011)
DOI: 10.1007/s11814-011-0095-4

Visible light-irradiated degradation of alachlor on Fe-TiO_2 with assistance of H_2O_2

Kitirote Wantala*, Pongtanawat Khemthong, Jatuporn Wittayakun***, and Nurak Grisdanurak****,†**

*Department of Chemical Engineering, Energy Management and Conservation Office, Faculty of Engineering, Khon Kaen University, Khon Kaen 40002, Thailand
**National Nanotechnology Center (NANOTEC), NSTDA, Pathumthani 12120, Thailand
***School of Chemistry, Suranaree University of Technology, Nakhon Ratchasima 30000, Thailand
****Department of Chemical Engineering, Faculty of Engineering, NCE for Environmental and Hazardous Waste Management, Thammasat University, Pathumthani 12120, Thailand
(*Received 19 August 2010 • accepted 10 April 2011*)

Abstract−0.1 Fe/Ti mole ratio of Fe-TiO_2 catalysts were synthesized via solvothermal method and calcined at various temperatures: 300, 400, and 500 °C. The calcined catalysts were characterized by XRD, N_2-adsorption-desorption, UV-DRS, XRF, and Zeta potential and tested for photocatalytic degradation of alachlor under visible light. The calcined catalysts consisted only of anatase phase. The BET specific surface area decreased with the calcination temperatures. The doping Fe ion induced a red shift of absorption capacity from UV to the visible region. The Fe-TiO_2 calcined at 400 °C showed the highest photocatalytic activity on degradation of alachlor with assistance of 30 mM H_2O_2 at pH 3 under visible light irradiation. The degradation fitted well with Langmuir-Hinshelwood model that gave adsorption coefficient and the reaction rate constant of 0.683 L mg^{-1} and 0.136 mg/L·min, respectively.

Keywords: Solvothermal, Fe-TiO_2, Visible Light, Alachlor, H_2O_2, Photocatalysis

INTRODUCTION

Alachlor (2-chloro-*N*-(2,6-diethylphenyl)-*N*-(methoxymethyl) acetamide) is a herbicide used to control annual grass and broadleaf weeds. After use, it can be absorbed in the soil and contaminate water reservoirs. Despite its low acute toxicity, alachlor has carcinogenic activity on humans [1]. The maximum concentration of alachlor in drinking water permitted by the United States Environmental Protection Agency (US-EPA) is 0.2 μg/L while the European maximum contaminant level (MCL) for pesticide in drinking water is 0.1 μg/L [2].

Because alachlor has widely been used in several countries including Thailand, its removal from water should be seriously considered and made. Alachlor can be degraded easily in the presence of photocatalysts and UV radiation. Titanium dioxide or titania (TiO_2) has been claimed to be the best catalyst, which can absorb photon to generate electrons and holes to react with organic compounds [3,4]. In general, the anatase phase of TiO_2 is a more active form compared to rutile. Various forms of TiO_2, including bulk nanoparticles (such as commercial P25), film immobilized on glass or nanoparticles dispersed on MCM-41, were applied for the treatments [5-7].

One limitation of TiO_2 is it can absorb UV light effectively but not visible light. This property can be improved by doping TiO_2 with ferric ion (Fe^{3+}) and the resulting materials showed an enhancement of photocatalytic reaction [8-10]. Such improvement was significant on the TiO_2 prepared by a solvothermal method, which exhibited a higher performance on decomposition of methyl orange than that of the commercial P25. The Fe^{3+} was proposed to capture electrons which restrain the recombination of electrons and holes [11].

Along with TiO_2, the presence of Fe^{3+} and hydrogen peroxide (H_2O_2) also improved the photodegradation of alachlor. The reaction between Fe^{3+} and H_2O_2 generates hydroxyl radicals and further accelerates degradation. In addition, H_2O_2 is an electron acceptor which is able to prevent the electron-hole recombination. However, an optimum amount of H_2O_2 should be determined to avoid an excessive amount which might decrease photocatalytic activity [12,13].

In this work, Fe^{3+} doped TiO_2 was synthesized by the solvothermal method and tested for photocatalytic degradation of alachlor under visible light with H_2O_2 assistance. The fixed loading of Fe on TiO_2 support (with the molar ratio of 0.1) was selected according to our previous investigation [10]. A calcination effect in the lower range of temperature (300-500 °C) was selected to prevent particle sintering and phase transformation. The effects of initial concentration (alachlor and H_2O_2) and solution pH were also included. The influence of physico-chemical properties (Fe-TiO_2) on photocatalytic activity was discussed.

EXPERIMENTAL

1. Catalyst Preparation

Titanium tetraisopropoxide (TTIP, 98%), isopropyl alcohol (IPA, 99.8%), ferric nitrate nonahydrate (Fe, 99%), polyethylene glycol (PEG, MW=20,000) were supplied by Merck and used without further purification.

The Fe-TiO_2 photocatalyst with Fe/Ti mole ratio of 0.1 was synthesized by solvolysis as described elsewhere [10]. The method was based on the reactant molar ratio of TTIP : PEG : IPA of 55.6 : 1.0 : 216.0 and PEG : IPA weight ratio of 1 : 10. TTIP and Fe were dissolved in a solution containing IPA and PEG and crystallized at 100 °C for three days. The obtained brown gel was dried at 80 °C overnight to produce the brown powder and calcined at the temperature

†To whom correspondence should be addressed.
E-mail: gnurak@engr.tu.ac.th

of 300, 400, and 500 °C for 3 h. The final product was ground and stored in a desiccator.

2. Catalyst Characterizations

The crystal phases and structures of the synthesized samples were analyzed by powder X-ray diffraction (XRD, Bruker D8) using a Cu K_α radiation. The chemical compositions of the calcined samples were analyzed by X-ray fluorescence spectroscopy (XRF, Siemens SRS3400) to confirm Fe/Ti molar ratio. The thermal property of the as-synthesized Fe-TiO_2 was analyzed simultaneously under air atmosphere by thermal gravimetric analysis (TGA, Shimadzu 50A). The temperature was ramped from 30 to 600 °C with a heating rate of 5 °C/min. BET specific surface area was obtained from a N_2 adsorption-desorption apparatus (Quantachrome Autosorb I). The band gap energy of the samples was determined by using UV-diffuse reflectance spectroscopy (UV-DRS, Hitashi UV3501) under the wavelength ranging from 250 to 800 nm and $BaSO_4$ was used as a standard. The surface potential of the prepared catalysts was determined by Zetasizer (Malvern ZS90).

3. Photocatalytic Degradation of Alachlor

Alachlor (99.5%) was supplied by Supelco (USA) and the synthetic alachlor solution was prepared by dissolving it in deionized water. The photocatalytic testing was conducted by suspending 50.0 mg of the Fe-TiO_2 catalyst in 200 mL alachlor solution which was irradiated by 500-W Xenon lamp (Shanghai DianGuang Device). The reactor was placed 50 cm away from the light source and the radiation was filtered by 1.0 M $NaNO_2$ to cut off wavelengths shorter than 400 nm. Flux intensity of 58 mW/cm^2 was detected inside the reactor and the reaction temperature was maintained at 25 °C. The initial concentration of H_2O_2 and alachlor was studied in range of 0-60 mM, and 2.5-19 ppm, respectively. In addition, the effect of initial pH was also studied at 3, 4, 7, and 9. Every 30 min, a sample was collected to determine the remaining amount of alachlor. The measurement was made by using an HPLC (Agilent Technologies 1200 series) coupled with a photodiode array detector, Agilent Technologies 1100 series pump and controller. The maximum absorption wavelength of 197 nm was used for the detection. The separation was performed by a Hypersil ODS C18 column (4.0×125 mm, 5 μm). The mobile phase consisting of a mixture of 60% acetonitrile and 40% HPLC-grade water was delivered at a flow rate of 1.0 mL/min with injection volume 20 μL. The absorbance was quantified by using a five-point standard calibration curve. The alachlor peak appeared at the retention time of 6.4 min.

RESULTS AND DISCUSSION

1. Characteristics of Catalysts

Fig. 1 shows the XRD patterns of Fe-TiO_2 catalysts calcined at 300, 400, and 500 °C, compared with commercial TiO_2 P25. Only the anatase phase was observed in all samples. The calcination temperatures in this study were not so high, resulting in no phase transformation from anatase to rutile phases. Based on the major peak at 26°, the average crystalline size of the anatase TiO_2 could be calculated using the Debye-Scherrer equation (Eq. (1)).

$$t = \frac{K\lambda}{\beta \cos\theta_B} \quad (1)$$

Where t is average crystallite size (nm), K is constant using 0.9, λ is X-ray wavelength (0.154 nm), β is the line broadening at half the maximum intensity in radians, θ_B is Bragg angle. The average crystallite sizes of the synthesized samples are listed in Table 1. The crystallite sizes of the samples were approximately 10 Å, much smaller than that of commercial TiO_2 (P25), ~20 Å.

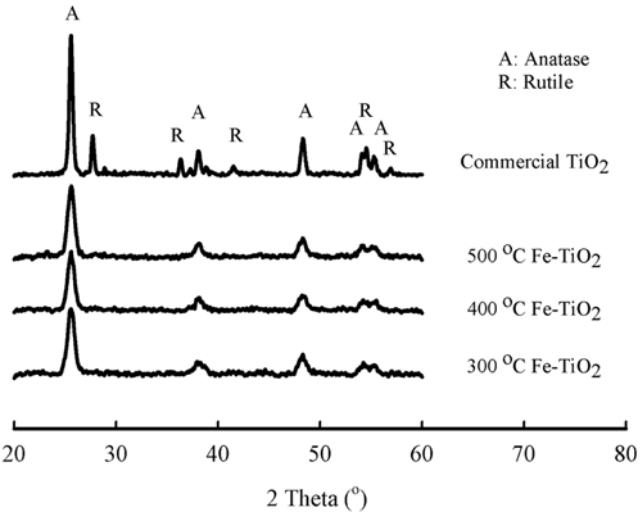

Fig. 1. XRD patterns of Fe-TiO_2 samples calcined at 300, 400, and 500 °C compared with commercial TiO_2 P25.

Table 1. Properties of synthesized catalysts

Nominal composition	S_{BET} (m^2g^{-1})	Titania crystalline size (nm)	Band edge wavelength (nm)	Band gap energy (eV)
Commercial TiO_2 P25	50	20.2	390	3.18
Fe-TiO_2 300 °C	90	9.4	470	2.64
Fe-TiO_2 400 °C	92	10.0	476	2.61
Fe-TiO_2 500 °C	52	9.9	481	2.58

Because the photocatalytic degradation of alachlor involves adsorption and reaction on the surface, the surface areas of the catalysts were measured and the results are listed in Table 1. All the synthesized catalysts under solvothermal technique had a surface area of approximately 52-90 m^2/g, higher than that of P25 which was 50 m^2/g.

According to the XRD results, the peaks identifying Fe_2O_3 (2θ= 24, 34, 36, 49, and 54) were not observed because the loading of Fe might be lower than the detection limit and be dispersed well in the titania structure. The Fe content in the catalyst determined by XRF was 0.09 and not different from the calculated value. Moreover, the same procedure revealed that Fe^{3+} ions were plausibly incorporated into the interstices or lattice sites and uniform dispersion in TiO_2 structure indicated by XANES and SEM element mapping, respectively, as presented in our previous report [10].

To understand the effects of the calcination temperature, TGA-DTA was analyzed. Fig. 2 shows percent weight loss and the heat flows in a material as a function of temperature. The weight loss appeared in two steps. The first range was from 30-130 °C with approximately 5% weight loss corresponding to the removal of residual acetone, isopropyl alcohol, and dry gel powder. The second region

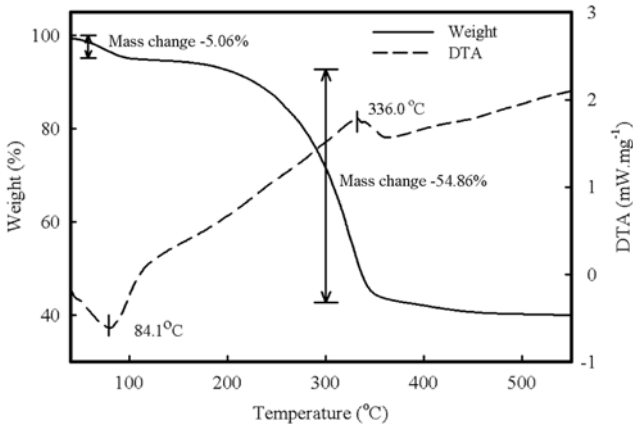

Fig. 2. Thermograph and DTA results of as-synthesized Fe-TiO_2.

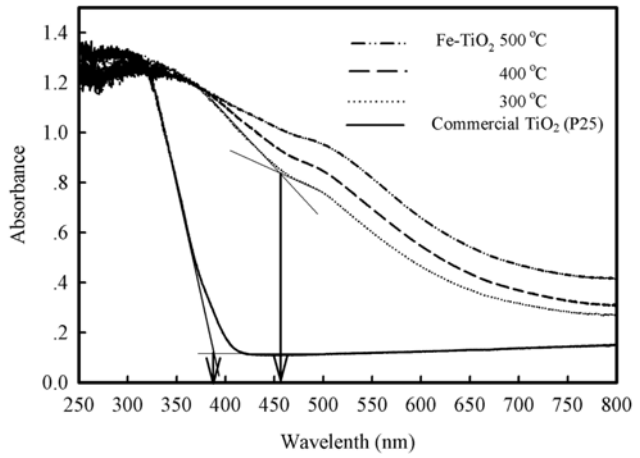

Fig. 3. UV-DR spectra of Fe-TiO_2 samples calcined at 300, 400, and 500 °C compared with commercial TiO_2 (P25).

was between 130-350 °C with about 55% weight loss attributed to the combustion of organic templates and nitrate ion. This was confirmed by the exothermic DTA peak at 336 °C. After that, there was no significant weight loss. The results indicated that the calcination at 400 °C would be sufficient to decompose the catalyst precursors to generate Fe-TiO_2. The data corresponded to BET surface area, listed in Table 1, that the samples calcined at 400 °C gave the highest BET surface area. The samples calcined at 300 °C still contained PEG or organic template and were not suitable for further application. The samples calcined at 500 °C had a lower surface area because the high temperature caused particle aggregation.

Fig. 3 shows the UV-visible spectra of calcined Fe-TiO_2 catalysts compared with P25. The diffuse reflectance spectra of all Fe-TiO_2 samples showed a red shift and the absorption in the visible region increased significantly. The shift increased with increasing the calcination temperature. Thus, doping TiO_2 with Fe improved the absorption of the Fe-TiO_2 and made it likely to be photocatalytically active under visible light. Similar red-shift characteristic was observed in Fe-doped titania nanorods and microspheres [14,15]. Yu et al. [14] stated that the absorptions in the visible region may be induced by a charge transfer transition of 3d electrons of Fe^{3+} to TiO_2 conduction band or a charge transfer transition between iron ions at 500 nm. Thus, the iron ions with incorporated into the lattice of TiO_2 and changed its electronic properties. The band gap energies of catalysts (Eg) were calculated by using Eq. (2) [16]:

$$Eg = \frac{hc}{\lambda \times 10^{-9}} \quad (2)$$

where h is Planck's constant (4.14×10^{-15} eV·s), c is the light velocity (2.99×10^{8} m/s) and λ is the band edge wavelength (nm) (such a band edge wavelength was obtained from an intersection of a tangent of the iron absorption peak onset (520 nm) and a steep line of UV absorption spectra, as shown in Fig. 3) [17,18]. The Eg of Fe-TiO_2 decreased when the samples were calcined at a higher temperature (Table 1). The Eg was approximately 2.6 eV, suggesting that these catalysts could be used under visible light (namely, wavelength >400 nm). The decrease in Eg was also observed in Fe-doped titania nanorods (2.97 eV) and microspheres (2.61 eV) [14,15].

2. Photocatalytic Degradation of Alachlor

As presented, high surface area of Fe-doped titania calcined at 400 °C was selected to degrade alachor by the photocatalytic process under several conditions, such as initial H_2O_2 concentration, initial solution pH and initial alachlor concentrations.

The effect of initial H_2O_2 concentrations was studied in the range of 0-60 mM. The test was carried out with initial concentration of alachlor of 5 ppm at pH 4.0, as shown in Fig. 4. The results showed that the photocatalytic reaction, without H_2O_2 dosage, produced the lowest activity. This indicates that energy emitted from visible light is unable to break O-H bond of a water molecule to yield OH^-. The results also showed that the initial concentrations of H_2O_2 enhanced the photocatalytic activity and optimized at the concentration of 30 mM. Regarding Eq. (3), H_2O_2 reacted with electrons and yielded •OH and OH^- and then OH^- would react with h^+ and transferred to •OH as shown in Eq. (4). Thus, H_2O_2 in the form of •OH can degrade alachlor in photocatalytic process. With a higher concentration of H_2O_2 than 30 mM, the photocatalytic activity was decreased. The overdose of H_2O_2 retarded the reaction rate because some hydroxyl radicals may have been consumed, which are explained in Eq. (5)-(6). Besides, the excess of H_2O_2 existing on the surface of catalysts

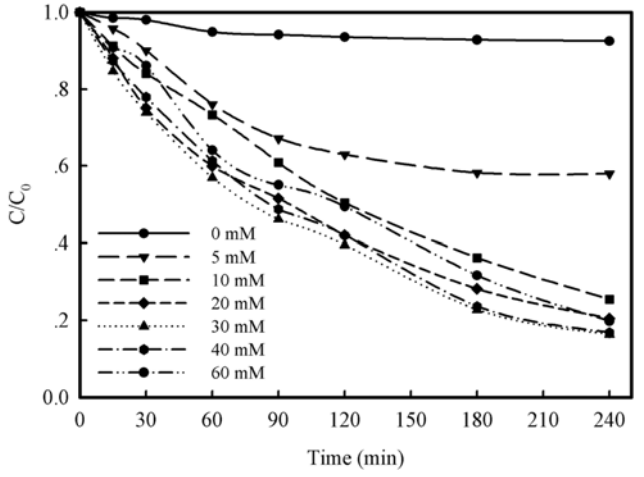

Fig. 4. Photodegradation of alachlor by Fe-TiO_2 as a function of concentration of H_2O_2 at condition: 5 ppm initial alachlor concentration and initial of pH 4.

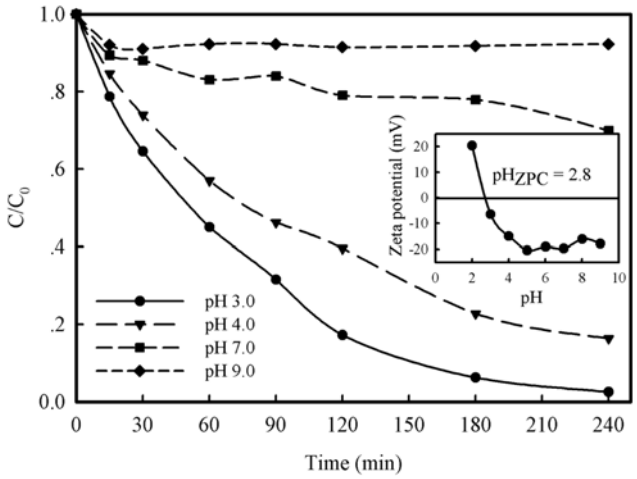

Fig. 5. Photodegradation of alachlor by Fe-TiO_2 as a function of initial pH at condition: 5 ppm initial alachlor concentration and 30 mM H_2O_2.

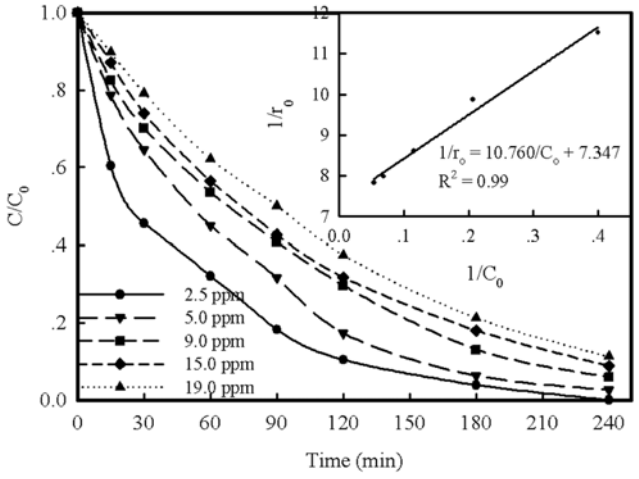

Fig. 6. Photodegradation of alachlor by Fe-TiO_2 as function of initial alachlor concentration at condition: 30 mM H_2O_2 and pH 3.

would obstruct alachlor species to adsorb on the surface.

$$e^- + H_2O_2 \rightarrow \bullet OH + OH^- \quad (3)$$

$$h^+ + OH^- \rightarrow \bullet OH \quad (4)$$

$$H_2O_2 + \bullet OH \rightarrow H_2O + \bullet HO_2 \quad (5)$$

$$HO_2 + \bullet OH \rightarrow H_2O + O_2 \quad (6)$$

A pH of aqueous medium has an influence on the stability of dispersion of Fe-TiO_2 powders. Thus, the effects of initial pH solutions were studied at 3, 4, 7, and 9 under the conditions of the initial concentration of alachlor of 5 ppm and H_2O_2 30 mM. Maximal photocatalytic activity was observed at pH 3 and decreased with increasing initial solution pH, as shown in Fig. 5. It could be explained by isoelectric charge of the material and the charge of alachlor solution. At pH 3, the surface of catalysts presented a state of neutral net surface charge (pH_{ZPC}=2.8, see the inserted figure in Fig. 5) and alachlor solution possessed more negative charges (pKa=0.67 at 25 °C). Conversely, at pH 4 or higher, both surface and solution would present mainly negative charges. Therefore, the interaction between alachlor species and the catalyst surfaces at pH 3 should be higher than that at pH 4 or higher.

Because this work was done in an acidic condition, it may have caused the leaching of Fe ions from the catalyst. Thus, Fe ions in aqueous solution were measured. The amount of Fe ions in the solution was not detected as indicated by the GF-AAS (Perkin Elmer, AAnalyst 800). This indicated that catalyst was impressively stable under a severe acidic condition.

The effects of initial alachlor concentrations were studied at 2.5, 5, 9, 15 and 19 ppm with initial concentration of H_2O_2 30 mM at pH 3.0. The results (Fig. 6) showed that the lower initial concentrations of alachlor gave the highest photocatalytic degradation efficiency. The results also showed that the reaction rate constants decreased with an increase in the initial alachlor concentrations. It was possible that, at higher concentrations, the alachlor adsorbed and covered the catalyst surface and resulted in deactivation that had been already discussed by Lee and co-workers [7].

To analyze the kinetic of photocatalytic oxidation, the data were fitted to the simple initial rate expression of the Langmuir-Hinshelwood (L-H) form as follows (Eq. (7)):

$$r_o = \frac{k_r K_{ad} C_o}{1 + K_{ad} C_o} \quad (7)$$

$$\frac{1}{r_o} = \frac{1}{K_{ad} k_r C_o} + \frac{1}{k_r} \quad (8)$$

where r_o, C_o, K_{ad} and k_r are the initial rate, the initial concentration of alachlor, the adsorption coefficient and the reaction rate constant, respectively. In general, K_{ad} and k_r can be calculated from the slope and interception of the plot of $1/r_o$ versus $1/C_o$ that corresponded to Eq. (8). The experimental data showed that the photocatalytic degradation of alachlor by all Fe-TiO_2 samples obeyed the simple rate expression of the L-H kinetics (see the inserted figure in Fig. 6) with different initial alachlor concentrations. As a result, K_{ad} and k_r were 0.683 L/mg and 0.136 mg/L.min, respectively. The photo-oxidation reaction of alachlor over Fe-TiO_2 mainly occurred at the catalyst surface.

Photodegradation is an electric-energy-intensive process. Accordingly, a figure-of-merit of the process based on electric energy consumption should be evaluated. Recently, the IUPAC has proposed the parameter for advanced oxidation processes (AOP) on the use of electrical energy. For the case of low pollutant concentration, the electrical energy per order (E_{EO}) is defined as the amount of electricity (kWh) required to minimize the concentration of a pollutant by 1st order of magnitude in every 1 m^3 of contaminated water. The E_{EO} (kWh/m^3/ order) can be calculated from the following Eq. (9):

$$E_{EO} = \frac{Pt1000}{V \log\left(\frac{C_o}{C}\right)} \quad (9)$$

The Eq. (9) can be arranged in linear form as follows in Eq. (10).

$$\log\left(\frac{C}{C_o}\right) = -\frac{1}{E_{EO}} \frac{Pt1000}{V} \quad (10)$$

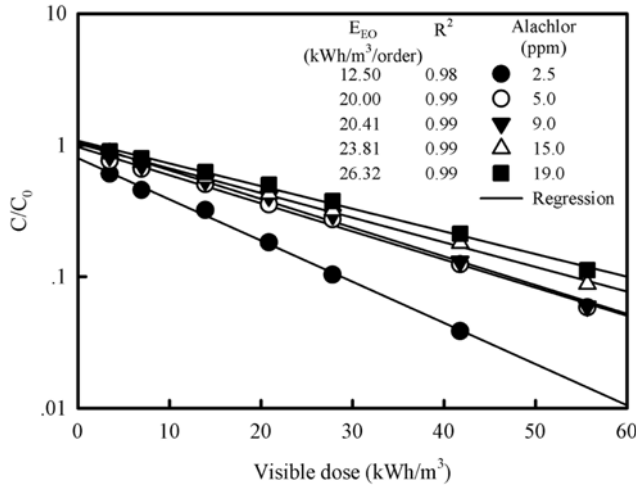

Fig. 7. (C/C$_o$) versus visible dose in the semilog scale, The E_{EO} values are calculated from the negative inverse slopes of the least-squares fit lines.

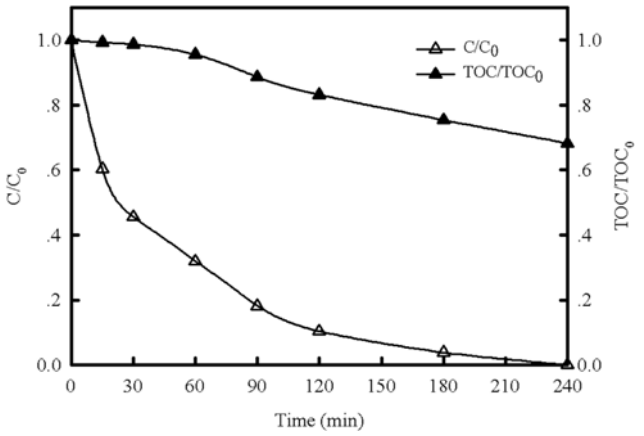

Fig. 8. Comparing TOC and photodegradation of alachlor by Fe-TiO$_2$ at 2.5 ppm initial concentration, 30 mM H_2O_2 and pH 3.

Where P is the power (kW) to the AOP system, t is the irradiation time (hour), V is the volume (L) of the water in the reactor, C_o and C are the initial and final alachlor concentrations [22]. E_{EO} can be calculated from the negative inverse slops of the plot of C/C_o versus visible dose (Pt1000/V) in the semilog scale that corresponded to Eq. (10) as shown in Fig. 7. The results showed that E_{EO} increased with increasing initial alachlor concentrations. E_{EO} increased from 12.50 to 26.32 kWh/m^3/order when alachlor concentrations increased from 2.5 to 19 ppm (see inserted table in Fig. 7).

Table 2 presents the potential of alachlor degradation under several conditions. As can be seen, the alachlor was highly degraded over P25 and UV irradiation. When the study was done in the visible light region, the degradation decreased 7 times. It may slightly be increased with $FeCl_3$ assistance. In this study, we improved the higher performance of alachlor degradation in the visible light by Fe incorporated into TiO_2 via solvothermal method.

With an initial concentration of 2.5 ppm of alachlor, the catalyst degraded the alachlor completely within 240 min. However, the organic intermediates were still present in the solution, as observed in the TOC profile (Fig. 8). The mineralization should take a longer time to be completed. Several pathways for the degradation of alachlor to small aliphatic organic end-products and then degraded to CO_2, H_2O, NH_3, NO_3^- and Cl^- are including dearomatization, dechlorination, hydroxylation, dealkylation, scission of the C-O bond, and N-dealkylation [19,23]. These pathways were the detoxification pro-

Table 2. Alachlor degradation by several conditions

Condition	Catalyst	Kinetic model	Rxn rate const; min^{-1}	Ref.
UV (300 nm)+4.94 mM H_2O_2 $C_{Alachlor}$ 5.93 ppm Catalyst loading 5 mg/L pH 6.0	TiO_2P25	pseudo-1st order	0.39	[5]
UV (300 nm)+10 mM $Na_2S_2O_8$ $C_{Alachlor}$ 50 ppm Catalyst loading 200 mg/L pH 2.8	TiO_2P25 $TiO_2$25+10 mg/L Fe^{3+}	Initial rate of TOC	0.0038 0.0122	[20]
UV (375 nm) $C_{Alachlor}$ 5 ppm Catalyst loading: 5 times of coating pH 5	TiO_2P25 thin film TiO_2P25 thin film+7.5 mg/L Fe^{3+}	pseudo-1st order	0.001 0.0018	[4]
Xenon lamp (without filter cutoff)+0.05% (v/v) H_2O_2 $C_{Alachlor}$ 30-60 ppb Catalyst loading 150 mg/L	TiO_2P25 TiO_2P25+15 mg/L $FeCl_3$	pseudo-1st order	0.053 0.065	[21]
Xenon lamp (400 nm cutoff)+30 mM H_2O_2 $C_{Alachlor}$ 2.5-19 ppm Catalyst loading 250 mg/L pH 3.0	Fe-TiO_2	L-H	0.093	This work

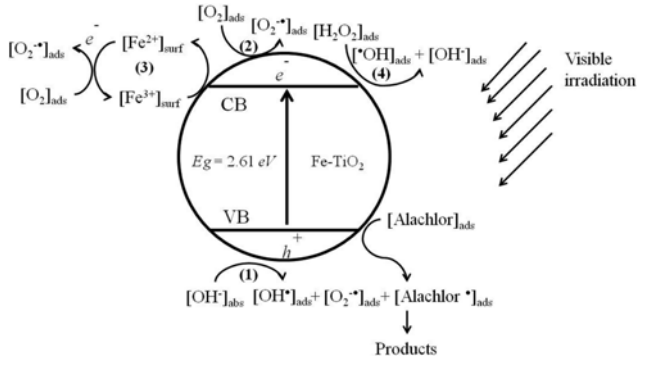

Fig. 9. The mechanism of alachlor degradation over Fe-TiO_2 photocatalyst under visible irradiation.

cess as reported by Mahmoodi and Arami [23].

Based on the results of the photocatalytic degradation of alachlor, the alachlor photodegradation mechanism under the visible irradiation can be proposed. The mechanism included four pathways, as shown in Fig. 8. Electrons in Fe-TiO_2 valence band were excited by the visible irradiation and moved to the conduction band. Path 1 shows OH^- on the surface of TiO_2 reacting with the holes and forming hydroxyl radicals (•OH), the main cause of the photodegradation of alachlor. Path 2 displays electrons in the conduction band reacting with the surface adsorbing O_2 molecules to yield O_2^-• radicals. Subsequently, the O_2^-• radicals reacted with adsorbed alachlor to break down their molecules. Additionally, Path 3 shows the Fe^{3+} on the surface of TiO_2 (photosensitization) being excited, bringing about efficient charge transfer in the composite samples. The Fe^{3+} particles could also act as electron traps. They could reduce electron recombination in the catalyst matrix, becoming Fe^{2+} species. Since Fe^{2+} was unstable, it would rapidly transfer an electron into O_2 molecules to yield more O_2^-• radicals. Therefore, the photocatalytic activity could be improved greatly.

Concerning Path 4, the effects of H_2O_2 as discussed above, led to oxidizing agent and reducing surface centers. In addition, the higher concentration of H_2O_2 would affect deleteriously to the performance.

CONCLUSIONS

The Fe-TiO_2, prepared by the solvothermal method and then calcination at different temperatures, showed that the physical and chemical properties of Fe-TiO_2 were affected by the calcination temperatures by means of the crystalline phase, crystalline size, surface area, and adsorption capacity. The catalyst calcined at 400 °C with the initial concentrations of H_2O_2 at 30 mM and pH 3.0 produced maximal the photocatalytic activity under visible light. The photocatalytic degradation rates corresponded to the Langmuir-Hinshelwood (L-H) kinetic model.

ACKNOWLEDGEMENTS

The authors would like to thank the National Research University Project of Thailand, Office of Higher Education Commission, and research fund from Suranaree University of Technology (SUT1-102-54-12-15) for their financial support.

REFERENCES

1. W. J. Lee, J. A. Hoppin, A. Blair, J. H. Lubin, M. Dosemeci, D. P. Sandler and M. C. R. Alavanja, *Am. J. Epidemiol.*, **159**, 373 (2004).
2. A. N. Benzbaruah, J. M. Thompson and B. J. Chishilm, *J. Environ. Sci. Health Part B.*, **44**, 518 (2009).
3. P. Atheba, D. Robert, A. Trokourev, D. Bamba and J. V. Weber, *Water Sci. Technol.*, **60**, 2187 (2009).
4. M. S. Kim, C. H. Ryu and B. W. Kim, *Water Res.*, **39**, 525 (2005).
5. C. C. Wong and W. Chu, *Environ. Sci. Technol*., **37**, 2310 (2003).
6. C. S. Ryu, M. S. Kim and B. W. Kim, *Chemosphere*, **53**, 765 (2003).
7. S. Artkla, K. Wantala, B. Srinameb, N. Grisdanurak, W. Klysubun and J. Wittayakun, *Korean J. Chem. Eng.*, **26**, 1556 (2009).
8. K. Wantala, D. Tipayarom, L. Laokiat and N. Grisdanurak, *React. Kinet. Catal. Lett.*, **97**, 249 (2009).
9. L. Deng, S. Wang, D. Liu, B. Zhu, W. Huang, S. Wu and S. Zhang, *Catal. Lett.*, **129**, 513 (2009).
10. K. Wantala, L. Loakiat, P. Khemthong, N. Grisdanurak and K. Fukaya, *J. Taiwan Inst. Chem. Eng.*, **41**, 612 (2010).
11. J. Wang, J. Li, L. Zhang, C. Li, Y. Xie, B. Liu, R. Xu and X. Zhang, *Catal. Lett.*, **130**, 551 (2009).
12. C. C. Wong and W. Chu, *Chemosphere*., **50**, 981 (2003).
13. D. D. Dionysiou, M. T. Suidan, I. Baudin and J. M. Lâýné, *Appl. Catal. B-Environ*., **50**, 259 (2004).
14. J. Yu, Q. Xiang and M. Zhou, *Appl. Catal. B-Environ.*, **90**, 595 (2009).
15. J. Li, J. Xu, W. L. Dai, H. Li and K. Fan, *Appl. Catal. B-Environ*., **85**, 162 (2009).
16. P. K. Surolia, R. J. Tayade and R. V. Jasra, *Ind. Eng. Chem. Res*., **46**, 6196 (2007).
17. X. H. Wang, J. G. Li, H. Kamiyama, M. Katida, N. Ohashi, Y. Moriyoshi and T. Ishigaki, *J. Am. Chem. Soc*., **127**, 10982 (2005).
18. A. B. Murphy, *Sol. Energ. Mater. Sol. C*., **91**, 1326 (2007).
19. W. Chu and C. C. Wong, *Ind. Eng. Chem. Res*., **43**, 5027 (2004).
20. M. H. Pérez, G. A. Penuela, M. I. Maldonado, O. Malato, P. Fernández-Ibáñez, I. Oller, W. Gernjak and S. Malato, *Appl. Catal. B-Environ*., **64**, 272 (2006).
21. G. A. Penuela and D. Barcelo, *J. Chromatogr. A.*, **754**, 187 (1996).
22. J. R. Bolton, K. G. Bircher, W. Tumas and C. A. Tolman, *Pure Appl. Chem*., **73**, 627 (2001).
23. N. M. Mahmoodi and M. Arami, *J. Alloy Compd*., **506**, 155 (2010).